Journal of the Persian Gulf
(Marine Science)/Vol. 6/No. 22/December 2015/16/13-28

Parametric Study of SCFs in Unstiffened Gap Tubular KT-joints of Offshore Structures under OPB Moment Loading

Ahmadi, Hamid*; Kordkarimi, Majid

Faculty of Civil Engineering, University of Tabriz, Tabriz, IR Iran

Received: April 2015 *Accepted: November 2015*

Abstract

In this paper, results extracted from a set of stress analyses performed on 46 FE models for unstiffened gap tubular KT-joints are presented and discussed. The main objective of the FE analyses, validated against experimental data, was to run a parametric investigation on the effects of geometrical characteristics of the joint on the values of the stress concentration factors (SCFs). The SCF is a key input parameter in the fatigue analysis and design of tubular joints commonly found in steel offshore structures such as jacket-type and jack-up platforms. Chord-side SCFs of central and outer braces were studied individually under four different types of out-of-plane bending (OPB) moment loads. After investigating the geometrical effects, a set of nonlinear parametric equations were developed for the computation of SCFs. Proposed equations, assessed according to the criteria recommended by the UK Department of Energy, can be reliably used for the fatigue calculations.

Keywords: *Fatigue, KT-joint, SCF, OPB moment*

1. Introduction

Jacket-type and jack-up platforms are among the most common offshore structures constructed for the exploitation of oil and natural gas resources below the seabed. The primary structural components of such platforms are steel tubular members. The interconnection among these members in which the prepared ends of brace members are welded onto the undisturbed surface of the chord member, is called a tubular joint (Fig. 1a).

Wave action produces fluctuating stresses in tubular joints that leads to fatigue damage accumulation and even causes structural failure without exceeding design wave loads. Significant stress concentrations at the vicinity of the welds are highly detrimental to the fatigue life of a tubular joint. For design purposes, a parameter called the stress concentration factor (SCF) is commonly used to quantify the stress concentration. Since, the SCF is a key input parameter for the fatigue analysis and design, its accurate calculation is clearly quite important.

The SCF, defined as the ratio of the local surface

* *Email: h-ahmadi@tabrizu.ac.ir*

stress at the brace/chord intersection to the nominal stress in the brace, exhibits considerable scatter depending on the joint geometry, loading type, weld size and type, and the position around the weld profile considered for the SCF determination. Under any specific loading condition, the SCF value along the weld toe of a tubular joint is mainly determined by the joint geometry. To study the behavior of tubular joints and to easily relate this behavior to the geometrical properties of the joint, a set of dimensionless geometrical parameters has been defined. Fig. 1b illustrates an unstiffened gap tubular KT-joint with the geometrical parameters τ, γ, β, ζ, α, and αB for chord and brace diameters D and d, and their corresponding wall thicknesses T and t. Critical positions along the weld toe of the brace/chord intersection for the calculation of SCFs in a tubular joint, i.e. saddle and crown for the central brace and saddle, crown toe and crown heel for the outer brace, have been shown in Fig. 1c.

(a) Tubular KT-joints in a jacket structure during fabrication

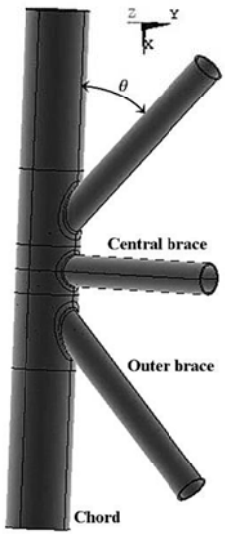

(b) Global geometry

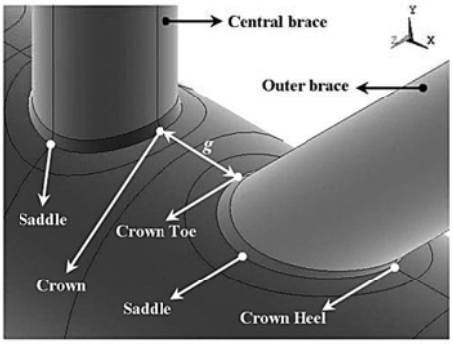

(c) Critical positions along the weld toe

D: Chord diameter;
d: Brace diameter;
T: Chord wall thickness;
t: Brace wall thickness;
L: Chord length;
l: Brace length;
g: Gap

$\beta = d/D$
$\gamma = D/2T$
$\tau = t/T$
$\zeta = g/D$
$\alpha = 2L/D$
$\alpha_B = 2l/d$

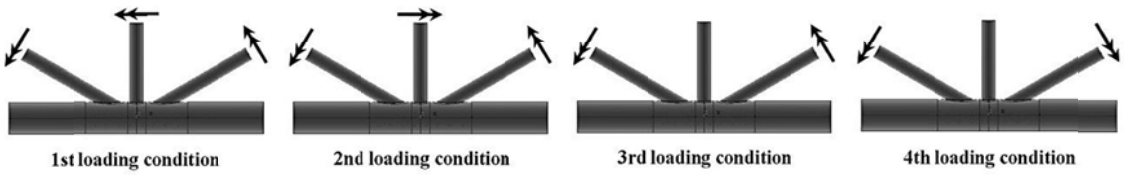

(d) Studied OPB load cases

Fig. 1: Geometrical notation for an unstiffened gap tubular KT-joint and studied out-of-plane bending (OPB) moment loadings

In this paper, results of numerical study of the SCFs in unstiffened gap tubular KT-joints are presented and discussed. In this research program, a set of parametric finite element (FE) stress analyses was carried out on 46 steel tubular KT-joint models subjected to four different types of out-of-plane bending (OPB) moment loading (Fig. 1d). All of these load cases can actually occur in a tubular joint of an offshore jacket structure depending on the wave incident angle, location of the joint, relative position of the wave crest, and design load combination. FE results were used to investigate the effect of geometrical parameters including τ (brace-to-chord thickness ratio), γ (chord wall slenderness ratio), β (brace-to-chord diameter ratio), and θ (outer brace inclination angle) on the SCFs at the saddle position. The crown positions were not studied. The reason is that, under the OPB moment loading, the nominal stress at these positions is zero and hence the SCF determination is not required. Based on the results of KT-joint FE models, validated against experimental data, a SCF database was prepared and six nonlinear parametric equations were developed for the computation of SCFs. The acceptability of these equations, derived based on nonlinear regression analyses, was evaluated according to the criteria recommended by the UK Department of Energy (1983).

2. Literature Review

There is a rich literature available on the study of SCFs in tubular joints: For unstiffened uniplanar joints, the reader is referred for example to Kuang et al. (1975), Wordsworth and Smedley (1978), Wordsworth (1981), Efthymiou and Durkin (1985), Efthymiou (1988), Hellier et al. (1990), Smedley and Fisher (1991), UK HSE OTH 354 (1997), and Karamanos et al. (2000) [for the SCF calculation at the saddle and crown positions of simple uniplanar T-, Y-, X-, K-, and KT-joints]; Gho and Gao (2004), Gao (2006), and Gao et al. (2007) [for the SCF determination in uniplanar overlapped tubular joints]; and Morgan and Lee (1998a, b), Chang and Dover (1999a, b), Shao (2004, 2007), Shao et al. (2009), Lotfollahi-Yaghin and Ahmadi (2010), and Ahmadi et al. (2011c) [for the study of the SCF distribution along the weld toe of various uniplanar joints].

For unstiffened multiplanar joints, the reader is referred to Karamanos et al. (1999) and Chiew et al. (2000) [for the SCF calculation in XX-joints]; Wingerde et al. (2001) [for the SCF determination in KK-joints]; Karamanos et al. (2002) [for the study of SCFs in DT-joints]; and Lotfollahi-Yaghin and Ahmadi (2011), Ahmadi et al. (2011a, 2012a) and Ahmadi and Lotfollahi-Yaghin (2012b) [for the comprehensive investigation of SCFs in two- and three-planar tubular KT-joints], among others.

For various types of stiffened joints, the reader is referred to Dharmavasan and Aaghaakouchak (1988), Aaghaakouchak and Dharmavasan (1990), Ramachandra et al. (1992), Nwosu et al. (1995), Ramachandra et al. (2000), Hoon et al. (2001), Myers et al. (2001), Woghiren and Brennan (2009), Ahmadi et al. (2012b, 2013), Ahmadi and Lotfollahi-Yaghin (2015), and Ahmadi and Zavvar (2015), among others.

For other SCF-related investigations such as probabilistic and reliability studies, the reader is referred for example to Fricke et al. (2008, 2013), Ahmadi et al. (2011b), Gaspar et al. (2011), Ahmadi and Lotfollahi-Yaghin (2012a, 2013), Ahmadi et al. (2015, 2016), and Ahmadi (2016).

3. Methodology

3.1. FE Modeling and Analysis

3.1.1. Geometry of Weld Profile

The weld sizes must be carefully included in the FE modeling. A number of research works has been carried out on the study of the weld effect. For example, the reader is referred to Lee and Wilmshurst

(1995), Cao et al. (1997) and Lee (1999), among others. It was found that the fatigue strength of the joint can be underestimated by 20% compared to the experimental data without considering the weld (Shao, 2004). In the present research, the welding size along the brace/chord intersection satisfies the AWS D 1.1 (2002) specifications. However, it should be noted that attempts to produce an improved as-welded profile often result in over-welding. Consequently, the actual weld size, typical of yard practice, is usually different from the nominal weld size recommended by AWS D 1.1 (2002) specifications. For the correction of SCFs to consider the actual position of the weld toe, the reader is advised to follow the recommendations of Section C 5.3.2(a) of API RP2A (2007).

The dihedral angle (ψ), that is an important parameter in determining the weld thickness, is defined as the angle between the chord and brace surface along the intersection curve. The dihedral angle at four typically important positions along the weld toe of central and outer braces can be determined as follows:

$$\psi = \begin{cases} \pi/2 & \text{Crown} \\ \pi - \cos^{-1}\theta & \text{Saddle} \\ \pi - \theta & \text{Toe} \\ \theta & \text{Heel} \end{cases} \quad (1)$$

where θ is the brace inclination angle (Fig. 1b).

Details of weld profile modeling according to AWS D 1.1 (2002) have been presented by Ahmadi et al. (2012a).

3.1.2. Applied Boundary Conditions

Fixity condition of the chord end in tubular joints of offshore structures ranges from almost fixed to almost pinned with generally being closer to almost fixed (Efthymiou, 1988). In practice, value of the parameter α in over 60% of tubular joints is in excess of 20 and is bigger than 40 in 35% of the joints (Smedley and Fisher, 1991). Changing the end restraint from fixed to pinned results in a maximum increase of 15% in the SCF at crown position for $\alpha = 6$ joints, and this increase reduces to only 8% for $\alpha = 8$ (Morgan and Lee, 1998b). In view of the fact that the effect of chord end restraints is only significant for joints with $\alpha < 8$ and high β and γ values, which does not commonly occur in practice, both chord ends were assumed to be fixed, with the corresponding nodes restrained.

As shown in Fig. 2a, only half of the entire KT-joint was required to be modeled due to the symmetry in geometry, material properties, and boundary conditions; and antisymmetry in loading; with respect to the XY-plane crossing the centroid of the chord. This allowed us to consider a reduced FE problem instead of the actual one. Thus, the order of the global stiffness matrix and total number of stiffness equations were reduced and computer solution time was substantially decreased. Since solid elements were used, the antisymmetry restraints were restricted to only translational displacements. This is because the solid elements do not have rotational degrees of freedom. Hence, for nodes located on the XY-plane crossing the centroid of the chord, the displacements were set to zero in the reduced structure ($d_x = 0$, $d_y = 0$). If shell elements had been used, in addition to the translational restraints, the rotation of the nodes normal to the XY-plane should also be set to zero ($\varphi_z = 0$).

3.1.3. Generated Mesh

ANSYS element type SOLID95 was used to model the chord, braces and the weld profiles. These elements have compatible displacements and are well-suited to model curved boundaries. The element is defined by 20 nodes having three degrees of freedom per node and may have any spatial orientation. Using this type of 3-D brick elements,

the weld profile can be modeled as a sharp notch. This method will produce more accurate and detailed stress distribution near the intersection in comparison with a simple shell analysis.

To guarantee the mesh quality, a sub-zone mesh generation method was used during the FE modeling. In this method, the entire structure is divided into several different zones according to the computational requirements. The mesh of each zone is generated separately and then, the mesh of entire structure is produced by merging the meshes of all the sub-zones. This method can easily control the mesh quantity and quality and avoid badly distorted elements. The mesh generated by this method for an unstiffened gap tubular KT-joint is shown in Fig. 2a and 2b.

As mentioned before, in order to determine the SCF, the stress at the weld toe should be divided by the nominal stress of the loaded brace. The stresses perpendicular to the weld toe at the extrapolation points are required to be calculated, in order to determine the stress at the weld toe position. To extract and extrapolate the stresses perpendicular to the weld toe, as shown in Fig. 2b, the region between the weld toe and the second extrapolation point was meshed in such a way that each extrapolation point was placed between two nodes located in its immediate vicinity. These nodes are located on the element-generated lines which are perpendicular to the weld toe ($X_{\perp}$ direction in Fig. 2d).

In order to make sure that the results of the FE analysis are not affected by the inadequate quality or the size of the generated mesh, convergence test was conducted and meshes with different densities were used in this test, before generating the 46 models. Based on the results of convergence test, the number of elements along the one half of brace/chord intersection (Fig. 2a) was selected to be 18. The number of elements through the chord and brace thickness was 2 and 1, respectively; and the number of elements on the surface, base, and back of the weld profile was 1, 2, and 3, respectively (Fig. 2b).

3.1.4. Analysis method and SCF computation procedure

For the SCF determination in tubular joints, static analysis of the linearly elastic type is recommended (N'Diaye et al., 2007). The Young's modulus and Poisson's ratio were taken to be 207 GPa and 0.3, respectively.

The weld-toe SCF at the saddle position is defined as:

$$\text{SCF} = \sigma_{\perp W} / \sigma_n \tag{2}$$

In Eq. (2), σ_n is the nominal stress of the OPB-loaded brace which is calculated as follows:

$$\sigma_n = \frac{32 d M_o}{\pi\left[d^4 - (d-2t)^4\right]} \tag{3}$$

where M_o is the out-of-plane bending moment.

To calculate the SCF, the stress at the weld toe position should be extracted from the stress field outside the region influenced by the local weld toe geometry. The location from which the stresses have to be extrapolated, extrapolation region, depends on the dimensions of the joint and on the position along the intersection. According to the linear extrapolation method recommended by IIW-XV-E (1999), the first extrapolation point must be at a distance of 0.4T from the weld toe, and the second point should lie at 1.0T further from the first point (Fig. 2c). In Eq. (2), $\sigma_{\perp W}$ is the extrapolated stress at the weld toe position which is perpendicular to the weld toe and is calculated by the following equation:

$$\sigma_{\perp W} = 1.4\sigma_{\perp E1} - 0.4\sigma_{\perp E2} \tag{4}$$

where $\sigma_{\perp E1}$ and $\sigma_{\perp E2}$ are the stresses at the first and second extrapolation points along the direction perpendicular to the weld toe, respectively.

The stress at an extrapolation point is obtained as follows:

$$\sigma_{\perp E} = \frac{\sigma_{\perp N1} - \sigma_{\perp N2}}{\delta_1 - \delta_2}\left(\Delta - \delta_2\right) + \sigma_{\perp N2} \tag{5}$$

where $\sigma_{\perp Ni}$ (i = 1 and 2) is the nodal stress at the immediate vicinity of the extrapolation point along

the direction perpendicular to the weld toe (Eq. (6)); δ_i (i = 1 and 2) is the distance between the weld toe and the considered node inside the extrapolation region (Eq. (7)); and Δ equals to 0.4T and 1.4T for the first and second extrapolation points, respectively (Fig. 2d).

$$\sigma_{\perp N} = \sigma_y m_1^2 + \sigma_z n_1^2 + 2\tau_{yz} m_1 n_1 \quad (6)$$

$$\delta = \sqrt{(x_w - x_n)^2 + (y_w - x_n)^2 + (z_w - x_n)^2} \quad (7)$$

In Eq. (7), (x_n ,y_n ,z_n) and (x_w, y_w, z_w) are the global coordinates of the considered node inside the extrapolation region and its corresponding node at the weld toe position, respectively. In Eq. (6), components of the stress tensor can be extracted from ANSYS analysis results; and m_1 and n_1 are transformation components calculated as follows:

$$m_1 = (y_w - y_n)/\delta \; ; \; n_1 = (z_w - z_n)/\delta \quad (8)$$

In order to facilitate the SCF calculation, above formulation was implemented in a *macro* developed by the ANSYS Parametric Design Language (APDL). The input data required to be provided by the user of the macro are the node number at the weld toe, the chord thickness, and the numbers of the nodes inside the extrapolation region. These nodes can be introduced using the Graphic user interface (GUI).

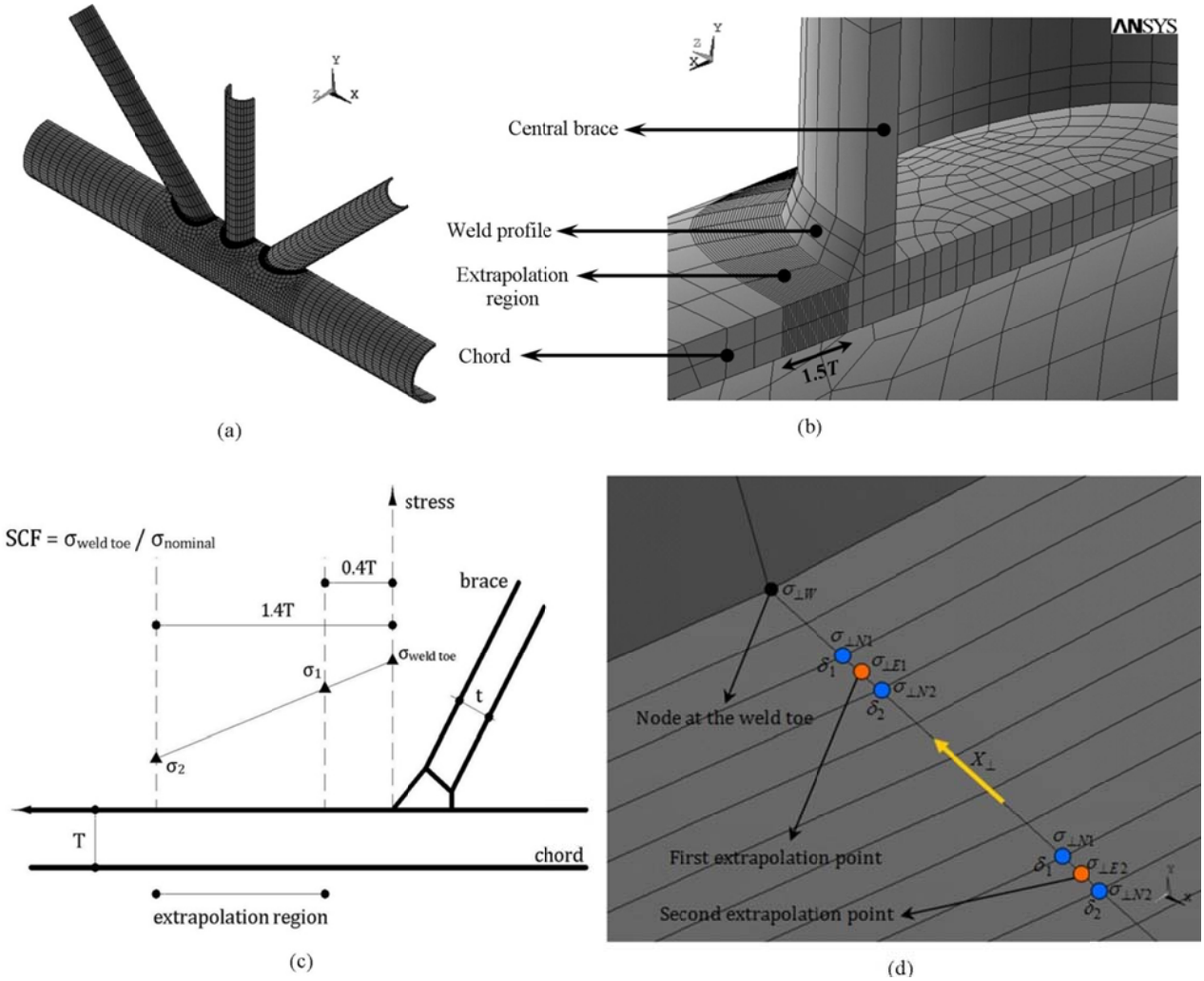

Fig. 2: (a) Global view of the generated mesh, (b) Mesh generated in the regions adjacent to the intersection, (c) Extrapolation method according to IIW-XV-E (1999), (d) Interpolations and extrapolations required to determine SCFs based on the stresses perpendicular to the weld toe

3.1.5. Verification of FE Results Using Experimental Measurements

To verify the developed FE modeling procedure, a validation FE model was generated and its results were compared with the results of experimental tests carried out by Ahmadi et al. (2013). Details of test setup and program are not presented here for the sake of brevity.

The specimen fabricated by Ahmadi et al. (2013) was tested under axial loading. In order to validate the FE models based on the data extracted from this experiment, the FE model of tested specimen was generated and analyzed under axial loading. The method of geometrical modeling (introducing the chord, braces, and weld profiles), the mesh generation procedure (including the selection of the element type and size), the analysis method, and the method of SCF extraction are the same for the validating model and the OPB-loaded joints used here for the parametric study. Hence, the verification of SCFs derived from axially-loaded FE model with corresponding experimental values lends some support to the validity of SCFs derived from OPB-loaded FE models. Moreover, in order to make sure that the OPB moment loading was correctly defined in ANSYS, nominal stresses obtained from the software were verified against the results of theoretical solid mechanics relations.

In Fig. 3, experimental data and FE results are compared. In this figure, the weld-toe SCF distribution along the central brace/chord intersection is presented. The polar angle (φ) along the 360˚ curve of the weld path is measured from the crown position. Hence, values of φ at the crown and saddle positions are 0˚/180˚/360˚ and 90˚/270˚, respectively.

The FE analysis predicts a stiffer structure than the actual one. This is expected, as the finite element model forces the structure into specific modes of displacement and effectively yields a stiffer model than the actual structure. This additional stiffness of the chord member yields to smaller deformation and consequently to lower SCFs of the chord member, compared to the experimental results. However, this does not mean that the results of FE models used for the parametric study are unconservative. The reason is that weld sizes in FE models used for the parametric study satisfy the AWS D 1.1 (2002) specifications and thus are smaller than weld sizes typically found in yard practice. Hence, as depicted in Fig. 3, the SCFs obtained from these models are higher than SCFs actually occurring in practice; and the FE results are even somewhat conservative.

As can be seen in Fig. 3, there is a good agreement between the test results and FE predictions. Hence, generated FE models can be considered to be accurate enough to provide valid results.

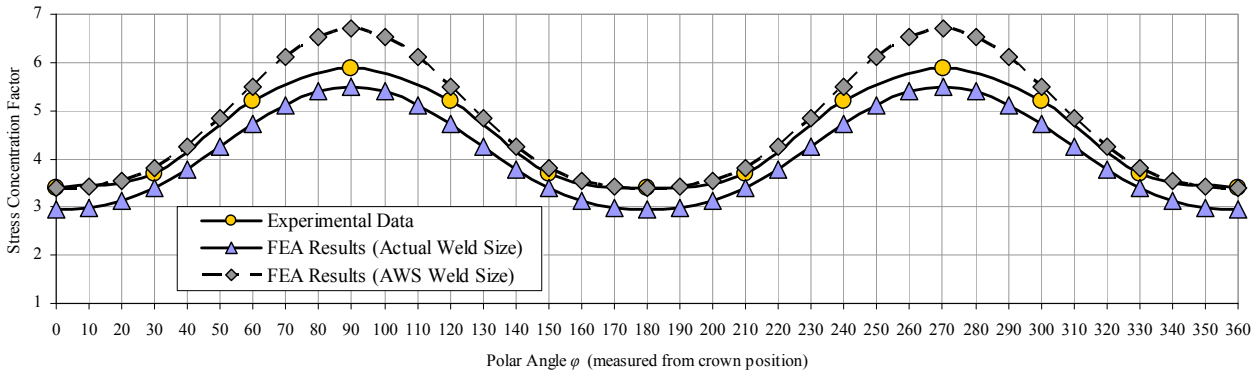

Fig. 3: Distribution of chord-side SCFs along the central brace/chord intersection of an unstiffened gap KT-joint: Comparing the results of experimental modeling and FE analysis

4. Results and Discussion

4.1. Effects of Geometrical Parameters on the SCFs

4.1.1. Details of Parametric Study

To study the SCFs in unstiffened gap KT-joints subjected to four types of OPB loading (Fig. 1d), 46 models were generated and analyzed using ANSYS. The aim was to investigate the effects of dimensionless geometrical parameters on the chord-side SCFs at the saddle position. As mentioned before, crown positions were not studied. The reason is that under the OPB loadings, the nominal stress at these positions is zero and hence the determination of SCFs is not required.

Different values assigned for parameters β, γ, τ, and θ are as follows: β = 0.4, 0.5, 0.6; γ = 12, 18, 24; τ= 0.4, 0.7, 1.0; and θ = 30˚, 45˚, 60˚. These values cover the practical ranges of dimensionless parameters typically found in tubular joints of offshore jacket structures. Providing that the gap between the central and outer braces is not very large, the relative gap (ζ = g / D) has no considerable effect on the SCF values in a tubular KT-joint. The validity range for this conclusion is $0.2 \le \zeta \le 0.6$ (Lotfollahi-Yaghin and Ahmadi, 2010). Hence, a typical value of ζ = 0.3 was designated for all joints. Sufficiently long chord greater than six chord diameters (i.e. $\alpha \ge 12$) should be used to ensure that the stresses at the brace/chord intersection are not affected by the chord's boundary conditions (Efthymiou, 1988). Hence, in this study, a realistic value of α = 16 was designated for all the models. The brace length has no effect on SCFs when the parameter αB is greater than the critical value (Chang and Dover, 1999a). In the present study, in order to avoid the effect of short brace length, a realistic value of α_B = 8 was assigned for all joints.

The 46 generated models span the following ranges of the geometric parameters:

$$0.4 \le \beta \le 0.6$$
$$12 \le \gamma \le 24 \qquad (9)$$
$$0.4 \le \tau \le 1.0$$
$$30^\circ \le \theta \le 60^\circ$$

4.1.2. Effect of the τ on the SCFs

This section presents the results of investigating the effect of the τ on the SCFs. In this study, the influence of parameters β, γ, and θ over the effect of the τ on SCFs was also investigated. The parameter τ is the ratio of brace thickness to chord thickness and the γ is the ratio of radius to thickness of the chord. Hence, the increase of the τ in models having constant value of the γ results in the increase of the brace thickness. For example, two charts are given in Fig. 4 depicting the change of chord-side SCFs of central and outer braces at the saddle position, under the 1st loading condition, due to the change in the value of the τ and the interaction of this parameter with the θ. Altogether, 24 comparative charts were used to study the effect of the τ and only two of them are presented here for the sake of brevity.

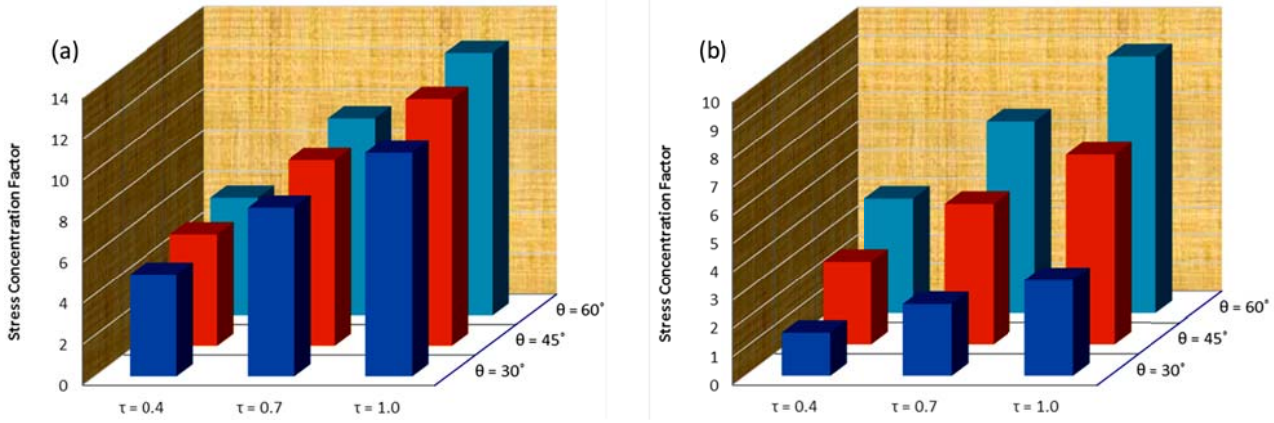

Fig. 4: Effect of the τ on the SCF values at the saddle position under the 1st OPB loading condition (β = 0.6, γ = 12): (a) Central brace, (b) Outer brace

Results indicated that the increase of the τ leads to the increase of SCFs at the saddle position under all studied OPB loading conditions. This result is not dependent on the values of other geometrical parameters. According to Fig. 4, it is evident that the effect of changing the parameter τ on the SCF values is greater than the effect of the parameter θ. It can also be observed that the central brace SCFs are bigger that the corresponding outer brace values.

4.1.3. Effect of the β on the SCFs

This section presents the results of investigating the effect of the β on the SCFs. In this study, the interaction of the β with the other geometrical parameters was also investigated. The parameter β is the ratio of brace diameter to chord diameter. Hence, the increase of the β in models having constant value of chord diameter results in the increase of brace diameter. Fig. 5 demonstrates the change of weld-toe SCFs at the saddle position, under the 1st loading condition, due to the change in the value of the β and the interaction of this parameter with the γ.

Through investigating the effect of the β on the SCFs, it can be concluded that the increase of the β leads to the increase of SCFs at the saddle position. This conclusion is not dependent on either the type of applied OPB load or the values of other geometrical parameters. It is also evident that, compared to the parameter β, the parameter γ is more effective in increasing the SCF values.

4.1.4. Effect of the γ on the SCFs

This section presents the results of investigating the effect of the γ on the SCFs. In this study, the influence of parameters β, τ, and θ over the effect of the γ on SCFs was also investigated. The parameter γ is the ratio of radius to thickness of the chord. Hence, the increase of the γ in models having constant value of the chord diameter means the decrease of chord thickness. For example, two charts are presented in Fig. 6 depicting the change of SCFs at the saddle position, due to the change in the value of the γ and the interaction of this parameter with the τ, under the 1st loading condition. Altogether, 24 comparative charts were used to study the effect of the γ and only two of them is presented here for the sake of brevity. It was observed that under all considered OPB loading conditions, the increase of the γ results in the increase of SCFs at saddle positions.

4.1.5. Effect of the θ on the SCFs

This section presents the results of studying the effect of the outer brace inclination angle θ on SCFs and its interaction with the other geometrical parameters. Two charts are given in Fig. 7, as an example, depicting the change of SCFs at the saddle position, under the 1st loading condition, due to the change in the value of θ and the interaction of this parameter with the β.

Through investigating the effect of the θ on the SCF values, it can be concluded that the increase of the θ leads to the increase of SCFs at saddle position. However, as expected, the amount of SCF change at the central brace is not considerable.

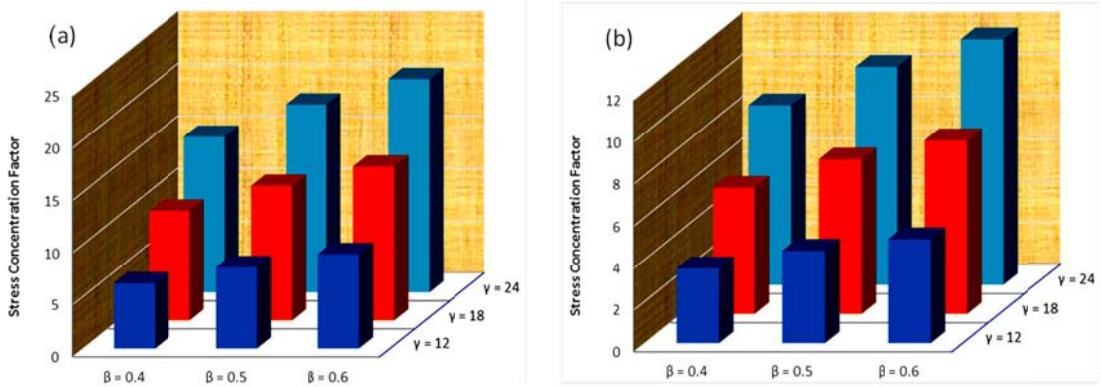

Fig. 5: Effect of the β on the SCF values at the saddle position under the 1st OPB loading condition (τ = 0.7, θ = 45°): (a) Central brace, (b) Outer brace

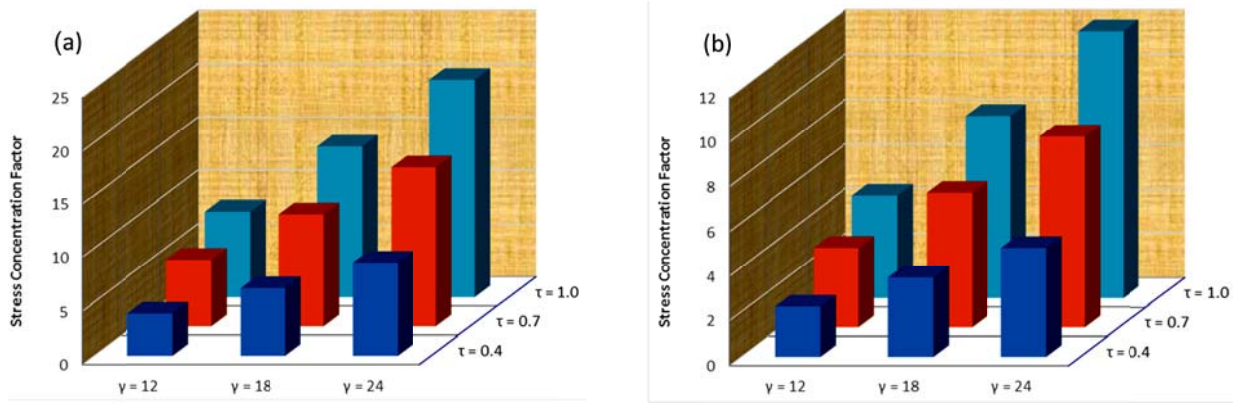

Fig. 6: Effect of the γ on the SCF values at the saddle position under the 1st OPB loading condition (β = 0.4, θ = 45°): (a) Central brace, (b) Outer brace

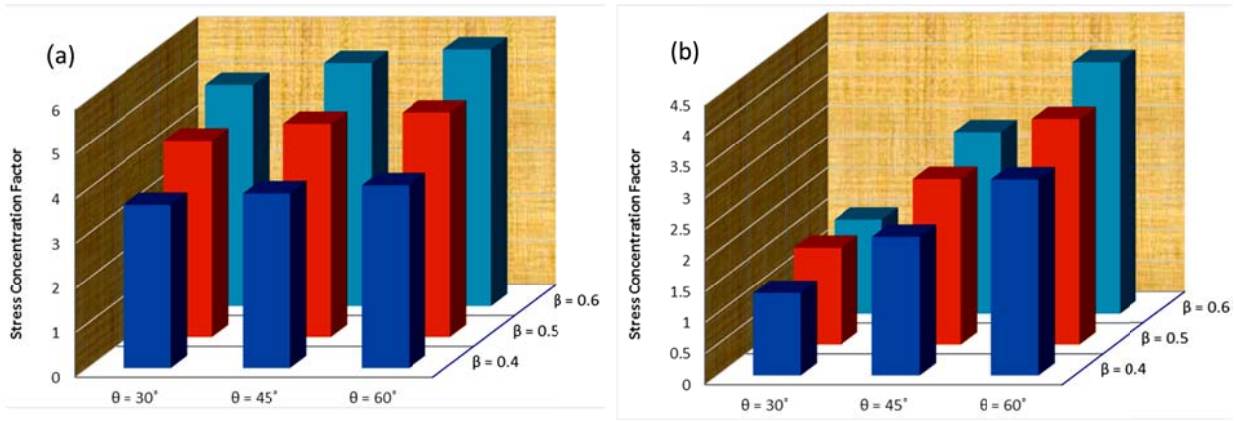

Fig. 7: Effect of the θ on the SCF values at the saddle position under the 1st OPB loading condition (τ = 0.4, γ = 12): (a) Central brace, (b) Outer brace

Derivation of parametric formulas for the SCF determination

Six individual parametric equations are proposed in the present paper to calculate the chord-side SCFs at the saddle position on the weld toe of central and outer braces in unstiffened gap tubular KT-joints subjected to four types of OPB loading.

Results of multiple nonlinear regression analyses performed by SPSS were used to develop parametric SCF design formulas. Values of dependent variable (i.e. SCF) and independent variables (i.e. β, γ, τ, and θ) constitute the input data imported in the form of a matrix. Each row of this matrix involves the information about the SCF value at the saddle position on the weld toe of central/outer brace in an unstiffened gap tubular KT-joint having specific geometrical properties. When the dependent and independent variables are defined, a model expression must be built with defined parameters. Parameters of the model expression are unknown coefficients and exponents. The researcher must specify a starting value for each parameter, preferably as close as possible to the expected final solution. Poor starting values can result in failure to converge or in convergence on a solution that is local (rather than global) or is physically impossible. Various model expressions must be built to derive a parametric equation having a high coefficient of determination (R^2) also called the coefficient of multiple correlation.

Following parametric equations are proposed, after performing a large number of nonlinear analyses, for the calculation of chord-side SCFs at the saddle position on the weld toe of central and outer braces in unstiffened gap tubular KT-joints subjected to four types of out-of-plane bending

(OPB) moment loading (Fig. 1d):

1st loading condition:

Central brace:

$$SCF=0.902\tau^{0.927}\gamma^{1.232}\beta^{0.808}\theta^{0.243} \quad R^2 = 0.998 \quad (10)$$

Outer brace:

$$SCF=0.505\tau^{0.970}\gamma^{1.297}\beta^{0.710}\theta^{1.318} \quad R^2 = 0.996 \quad (11)$$

2nd loading condition:

Central brace:

$$SCF=0.519\tau^{0.919}\gamma^{1.007}\beta^{0.224}\theta^{-0.410} \quad R^2 = 0.990 \quad (12)$$

Outer brace:

$$SCF=0.432\tau^{0.951}\gamma^{1.092}\beta^{0.335}\theta^{1.739} \quad R^2 = 0.993 \quad (13)$$

3rd loading condition:

Outer brace:

$$SCF=0.488\tau^{0.926}\gamma^{1.068}\beta^{0.314}\theta^{1.413} \quad R^2 = 0.994 \quad (14)$$

4th loading condition:

Outer brace:

$$SCF=0.478\tau^{0.943}\gamma^{1.090}\beta^{0.356}\theta^{1.425} \quad R^2 = 0.994 \quad (15)$$

The parameter θ should be inserted in radians in Eqs. (10)–(15). Values obtained for R^2 are quite high indicating the accuracy of the fit. The validity ranges of dimensionless geometrical parameters for the developed equations have been given in Eq. (9).

The UK Department of Energy (1983) recommends the following assessment criteria regarding the applicability of the commonly used SCF parametric equations (P/R stands for the ratio of the *predicted* SCF from a given equation to the *recorded* SCF from test or analysis):

- For a given dataset, if % SCFs under-predicting $\leq$ 25%, i.e. [%P/R < 1.0] $\leq$ 25%, and if % SCFs considerably under-predicting $\leq$ 5%, i.e. [%P/R < 0.8] $\leq$ 5%, then accept the equation. If, in addition, the percentage SCFs considerably over-predicting $\geq$ 50%, i.e. [%P/R > 1.5] $\geq$50%, then the equation is regarded as generally conservative.
- If the acceptance criteria is nearly met i.e. 25% < [%P/R < 1.0] $\leq$ 30%, and/or 5% < [%P/R < 0.8] $\leq$ 7.5%, then the equation is regarded as borderline and engineering judgment must be used to determine acceptance or rejection.
- Otherwise, reject the equation as it is too optimistic.

In view of the fact that for a mean fit equation, there is always a large percentage of under-prediction, the requirement for joint under-prediction, i.e. P/R < 1.0, can be completely removed in the assessment of parametric equations (Bomel Consulting Engineers, 1994). Assessment results according to the UK Department of Energy (1983) criteria are presented in Table 1. As can be seen in this table, all of the proposed equations satisfy the criteria recommended by UK Department of Energy.

In order to assess the reliability of proposed equations, results of Eqs. (10) and (11) which were derived to calculate the chord-side SCFs of central and outer braces under the 1st OPB load case (Fig. 1d) have been compared with the SCFs obtained from the equations proposed by Efthymiou (1988) for KT-joints subjected to the same OPB loading condition. Efthymiou's equations can also be found in API RP2A (2007) and UK HSE OTH 354 (1997). Results of this comparison, for 36 joints with different geometrical parameters, are presented in Fig. 8. In order to measure the difference between the results of Efthymiou's equations and the equations proposed in the present research, Normalized Root Mean Square Error (NRMSE) and Normalized Mean Absolute Error (NMAE) were calculated based on the following formulas:

$$NRMSE = \frac{1}{\left(SCF_{Efthymiou}\right)_{\max} - \left(SCF_{Efthymiou}\right)_{\min}} \sqrt{\frac{\sum_{i=1}^{n}\left(\left(SCF_{Efthymiou}\right)_i - \left(SCF_{present}\right)_i\right)^2}{n}} \quad (16)$$

$$MAE = \frac{1}{n\left(\left(SCF_{Efthymiou}\right)_{\max} - \left(SCF_{Efthymiou}\right)_{\min}\right)} \sum_{i=1}^{n}\left|\left(SCF_{Efthymiou}\right)_i - \left(SCF_{present}\right)_i\right| \quad (17)$$

where, $SCF_{Efthymiou}$ and $SCF_{present}$ are the SCF values obtained from the Efthymiou's equations and the equations proposed in the present paper, respectively. Results of the assessment are presented in Table 2. It can be seen that, except in one case, the differences are less than 10%. It can also be observed that even in this exceptional case, that is related to the central brace SCFs, Eq. (10) is more conservative compared to Efthymiou's equation and consequently,

its application will be safe. Fig. 8 and Table 2 indicate that, for both central and outer braces, there is a good agreement between the results of equations proposed by Efthymiou and the present research.

Table 1: Evaluation of proposed equations according to the UK Department of Energy (1983) criteria

Loading Condition	Brace	Equation	UK DoE Conditions			Decision
			$\%P/R < 1.0$	$\%P/R < 0.8$	$\%P/R > 1.5$	
1st	Central	Eq. (10)	64% > 25%	0% < 5% OK.	0% < 50% OK.	Accept
1st	Outer	Eq. (11)	55% > 25%	0% < 5% OK.	0% < 50% OK.	Accept
2nd	Central	Eq. (12)	58% > 25%	0% < 5% OK.	0% < 50% OK.	Accept
2nd	Outer	Eq. (13)	61% > 25%	2% < 5% OK.	0% < 50% OK.	Accept
3rd	Outer	Eq. (14)	55% > 25%	0% < 5% OK.	0% < 50% OK.	Accept
4th	Outer	Eq. (15)	50% > 25%	0% < 5% OK.	0% < 50% OK.	Accept

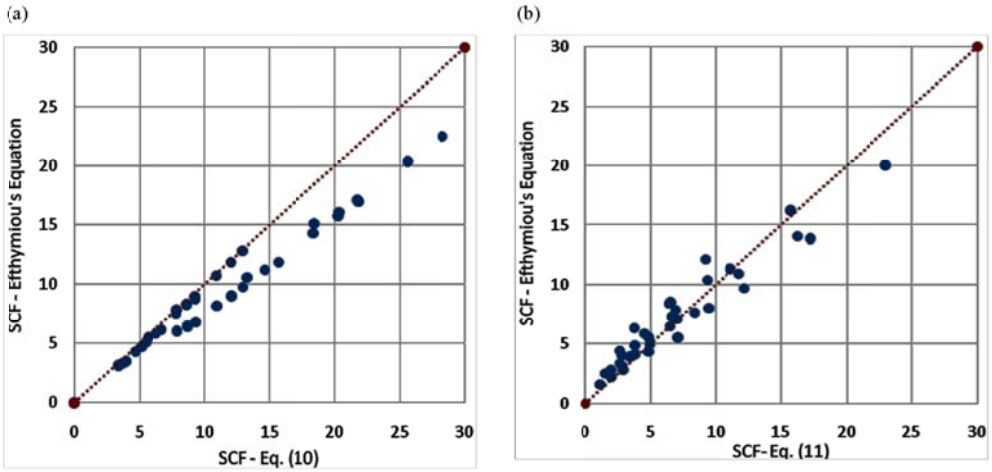

Fig. 8: Comparison of SCFs obtained from equations proposed by Efthymiou (1988) and present research – 1st OPB load case (Fig. 1d): (a) central brace chord-side SCFs; (b) outer brace chord-side SCFs

Table 2: The difference between the SCFs obtained from the equations proposed by Efthymiou (1988) and the present research

Equation	Characteristics	NRMSE	NMAE
Eq. (10)	For central brace SCFs under the 1st OPB load case (Fig. 1d), R^2 = 0.998	13.2%	9.6%
Eq. (11)	For outer brace SCFs under the 1st OPB load case (Fig. 1d), R^2 = 0.996	7.9%	6.1%

5. Conclusions

Effects of geometrical parameters on the chord-side SCFs at the saddle position in tubular KT-joints of unstiffened gap type were investigated. Altogether 46 FE models were generated and analyzed under four types of out-of-plane bending (OPB) moment loads leading to a total of 184 stress analyses. Results verified using experimental data were used to investigate the SCFs of central and outer braces individually. A set of SCF parametric equations was also proposed for the fatigue calculations. Main conclusions can be summarized as follows:

The central brace SCFs are bigger than the corresponding outer brace values. The increase of the τ and/or γ leads to the increase of SCFs at the saddle position. The effect of changing the parameter τ on the SCF values is greater than the effect of the parameter θ. The increase of the β leads to the increase of SCFs at the saddle position. Compared to the parameter β, the parameter γ is more effective in increasing the SCF values. The increase of the θ

leads to the increase of SCFs at saddle position. However, as expected, the amount of SCF change at the central brace is not considerable. These results are not dependent on either the type of OPB loading or the values of other geometrical parameters.

Both central- and outer-brace SCFs under the axial loading are quite bigger than the corresponding values under OPB loading conditions. This implies that if the SCF design equations developed for the unstiffened gap KT-joints under the axial loading are used for the SCF calculation in the OPB-loaded joints, result will be unrealistic and highly conservative. Hence, it is necessary to establish SCF formulas for OPB-loaded joints of this type. High coefficients of determination, the satisfaction of acceptance criteria recommended by the UK Department of Energy, and the good agreement with the existing well-known equations, guarantee the accuracy of six parametric equations proposed in the present paper. Hence, the developed formulas can reliably be used for the fatigue calculations.

Acknowledgements

The authors would like to thank Mr. Esmaeil Zavvar for his help during the numerical study.

References

Aaghaakouchak AA, Dharmavasan S., 1990. Stress analysis of unstiffened and stiffened tubular joints using improved finite element model of intersection. Proceedings of the Ninth International Conference on Offshore Mechanics and Arctic Engineering, Vol. III, Part A, Houston (TX), US.

Ahmadi H., 2016. A probability distribution model for SCFs in internally ring-stiffened tubular KT-joints of offshore structures subjected to out-of-plane bending loads. Ocean Engineering. 116:184–199.

Ahmadi H, Lotfollahi-Yaghin MA, Aminfar MH., 2011a. Distribution of weld toe stress concentration factors on the central brace in two-planar CHS DKT-connections of steel offshore structures. Thin-Walled Structures. 49:1225–1236.

Ahmadi H, Lotfollahi-Yaghin MA, Aminfar MH. 2011b, Effect of stress concentration factors on the structural integrity assessment of multi-planar offshore tubular DKT-joints based on the fracture mechanics fatigue reliability approach. Ocean Engineering 38:1883−1893.

Ahmadi H, Lotfollahi-Yaghin MA, Aminfar MH., 2011c. Geometrical effect on SCF distribution in uni-planar tubular DKT-joints under axial loads. Journal of Constructional Steel Research. 67:1282–1291.

Ahmadi H, Lotfollahi-Yaghin MA, Aminfar MH. 2012a., The development of fatigue design formulas for the outer brace SCFs in offshore three-planar tubular KT-joints. Thin-Walled Structures. 58:67–78.

Ahmadi H, Lotfollahi-Yaghin MA, Shao YB, Aminfar MH., 2012b. Parametric study and formulation of outer-brace geometric stress concentration factors in internally ring-stiffened tubular KT-joints of offshore structures. Applied Ocean Research. 38:74−91.

Ahmadi H, Lotfollahi-Yaghin MA, Shao YB., 2013. Chord-side SCF distribution of central brace in internally ring-stiffened tubular KT-joints: A geometrically parametric study. Thin-Walled Structures. 70:93−105.

Ahmadi H, Lotfollahi-Yaghin MA., 2012a. A probability distribution model for stress concentration factors in multi-planar tubular DKT-joints of steel offshore structures. Appl Ocean Research. 34:21−32.

Ahmadi H, Lotfollahi-Yaghin MA., 2013. Effect of SCFs on S–N based fatigue reliability of multi-planar tubular DKT-joints of offshore jacket-type structures. Ships Offshore Structures. 8:55−72.

Ahmadi H, Lotfollahi-Yaghin MA., 2012b. Geometrically parametric study of central brace SCFs in offshore three-planar tubular KT-joints. Journal of Construction Steel Research. 71:149–161.

Ahmadi H, Lotfollahi-Yaghin MA., 2015. Stress concentration due to in-plane bending (IPB) loads in ring-stiffened tubular KT-joints of offshore structures: Parametric study and design formulation. Applied Ocean Research. 51:54–66.

Ahmadi H, Zavvar E., 2015. Stress concentration factors induced by out-of-plane bending loads in ring-stiffened tubular KT-joints of jacket structures. Thin-Walled Structures. 91:82–95.

Ahmadi H. Mohammadi AH, Yeganeh A. Zavvar E., 2016. Probabilistic analysis of stress concentration factors in tubular KT-joints reinforced with internal ring stiffeners under in-plane bending loads. Thin-Walled Structures. 99:58–75.

Ahmadi H. Mohammadi AH, Yeganeh A., 2015. Probability density functions of SCFs in internally ring-stiffened tubular KT-joints of offshore structures subjected to axial load. Thin-Walled Structures. 94:485–499.

American Petroleum Institute (API). 2007. Recommended practice for planning, designing and constructing fixed offshore platforms: Working stress design: RP2A-WSD. 21st Edition, Errata and Supplement 3, Washington DC, US.

American Welding Society (AWS)., 2002. Structural welding code: AWS D 1.1. Miami (FL): American Welding Society.

Bomel Consulting Engineers. 1994. Assessment of SCF equations using Shell/KSEPL finite element data. C5970R02.01 REV C.

Cao JJ, Yang GJ, Packer JA., 1997. FE mesh generation for circular tubular joints with or without cracks. Proceedings of the 7th International Offshore and Polar Engineering Conference, Honolulu (HI), US.

Chang E, Dover WD., 1999a. Parametric equations to predict stress distributions along the intersection of tubular X and DT-joints. International Journal of Fatigue. 21:619–635.

Chang E, Dover WD. 1999b. Prediction of stress distributions along the intersection of tubular Y and T-joints. International Journal of Fatigue. 21:361–381.

Chiew SP, Soh CK, Wu NW. 2000. General SCF design equations for steel multiplanar tubular XX-joints. International Journal of Fatigue. 22:283–293.

Dharmavasan S, Aaghaakouchak, AA. 1988. Stress concentrations in tubular joints stiffened by internal ring stiffeners. Proceedings of the Seventh International Conference on Offshore Mechanics and Arctic Engineering, Houston (TX), US.

Efthymiou M., Durkin S., 1985. Stress concentrations in T/Y and gap/overlap K-joints. Proceedings of the Conference on Behavior of Offshore Structures, Delft, Netherlands.

Efthymiou M., 1988. Development of SCF formulae and generalized influence functions for use in fatigue analysis. Offshore Tubular Joints (OTJ) 88, Surrey, UK.

Fricke W, Bollero A, Chirica I, Garbatov Y, Jancart F, et al., 2008. Round robin study on structural hot-spot and effective notch stress analysis. Ships Offshore Struct. 3(4):335–345.

Fricke W, Codda M, Feltz O, Garbatov Y, Remes H, et al., 2013. Round robin study on local stress and fatigue assessment of lap joints and doubler plates. Ships Offshore Structures. 8(6):621–627.

Gao F, Shao YB, Gho WM. 2007. Stress and strain concentration factors of completely overlapped tubular joints under lap brace IPB load. Journal Construction Steel Research. 63:305–316.

Gao F. 2006., Stress and strain concentrations of completely overlapped tubular joints under lap brace OPB load. Thin-Walled Struct. 44:861–871.

Gaspar B, Garbatov Y, Guedes Soares C. 2011. Effect of weld shape imperfections on the structural hot-spot stress distribution. Ships Offshore Structures. 6(1-2):145–159.

Gho WM, Gao F., 2004. Parametric equations for stress concentration factors in completely overlapped tubular K(N)-joints. Journal of Construction Steel Research. 60:1761–1782.

Hellier AK, Connolly M, Dover WD., 1990. Stress concentration factors for tubular Y and T-joints.

International Journal of Fatigue. 12:13–23.

Hoon KH, Wong LK, Soh AK., 2001. Experimental investigation of a doubler-plate reinforced tubular T-joint subjected to combined loadings. Journal of Constraction Steel Research 57:1015–1039.

IIW-XV-E., 1999. Recommended fatigue design procedure for welded hollow section joints, IIW Docs, XV-1035-99/XIII-1804-99. Paris (France): International Institute of Welding.

Karamanos SA, Romeijn A, Wardenier J., 2002. SCF equations in multi-planar welded tubular DT-joints including bending effects. Mar Struct. 15:157–173.

Karamanos SA, Romeijn A, Wardenier J., 1990. Stress concentrations in multi-planar welded CHS XX-connections. J Constr Steel Res. 50:259–282.

Karamanos SA, Romeijn A, Wardenier J., 2000. Stress concentrations in tubular gap K-joints: mechanics and fatigue design. Eng Struct. 22:4–14.

Kuang JG, Potvin AB, Leick RD., 1975. Stress concentration in tubular joints. Proceedings of the Offshore Technology Conference, Paper OTC 2205, Houston (TX), US.

Lee MK, Wilmshurst SR., 1995. Numerical modeling of CHS joints with multiplanar double-K configuration. J Constr Steel Res. 32:281–301.

Lee MMK., 1999. Strength, stress and fracture analyses of offshore tubular joints using finite elements. J Constr Steel Res. 51:265–286.

Lotfollahi-Yaghin MA, Ahmadi H., 2010. Effect of geometrical parameters on SCF distribution along the weld toe of tubular KT-joints under balanced axial loads. Int J Fatigue. 32:703–719.

Lotfollahi-Yaghin MA, Ahmadi H., 2011. Geometric stress distribution along the weld toe of the outer brace in two-planar tubular DKT-joints: Parametric study and deriving the SCF design equations. Mar Struct. 24:239–260.

Morgan MR, Lee MMK., 1998a. Parametric equations for distributions of stress concentration factors in tubular K-joints under out-of-plane moment loading. Int J Fatigue. 20:449–461.

Morgan MR, Lee MMK., 1998b. Prediction of stress concentrations and degrees of bending in axially loaded tubular K-joints. J Constr Steel Res. 45(1):67–97.

Myers PT, Brennan FP, Dover WD., 2001. The effect of rack/rib plate on the stress concentration factors in jack-up chords. Mar Struct. 14:485–505.

N'Diaye A, Hariri S, Pluvinage G, Azari Z., 2007. Stress concentration factor analysis for notched welded tubular T-joints. Int J Fatigue. 29:1554–1570.

Nwosu DI, Swamidas ASJ, Munaswamy K., 1995. Numerical stress analysis of internal ring-stiffened tubular T-joints. J Offshore Mech Arctic Eng. 117:113–125.

Ramachandra DS, Gandhi P, Raghava G, Madhava Rao AG. 2000. Fatigue crack growth in stiffened steel tubular joints in seawater environment. Eng Struct. 22:1390–1401.

Ramachandra Murthy DS, Madhava Rao AG, Ghandi P, Pant PK., 1992. Structural efficiency of internally ring stiffened steel tubular joints. ASCE J Struct Eng. 118(11):3016–3035.

Shao YB, Du ZF, Lie ST. 2009. Prediction of hot spot stress distribution for tubular K-joints under basic loadings. J Constr Steel Res. 65:2011–2026.

Shao YB. 2004. Fatigue behaviour of uni-planar CHS gap K-joints under axial and in-plane bending loads. PhD Thesis, School of Civil & Environmental Engineering, Nanyang Technological University, Singapore.

Shao YB. 2007. Geometrical effect on the stress distribution along weld toe for tubular T- and K-joints under axial loading. J Constr Steel Res. 63:1351–1360.

Shao YB. 2004. Proposed equations of stress concentration factor (SCF) for gap tubular K-joints subjected to bending load. Int J Space Struct. 19:137–147.

Smedley P, Fisher P., 1991. Stress concentration factors for simple tubular joints. Proceedings of the International Offshore and Polar Engineering Conference (ISOPE), Edinburgh, UK.

UK Department of Energy., 1983. Background notes

to the fatigue guidance of offshore tubular joints. London (UK): Department of Energy.

UK Health and Safety Executive. 1997. OTH 354: stress concentration factors for simple tubular joints-assessment of existing and development of new parametric formulae. Prepared by Lloyd's Register of Shipping, London (UK): Health and Safety Executive.

Wingerde AM, Packer JA, Wardenier J., 2001. Simplified SCF formulae and graphs for CHS and RHS K- and KK-connections. Journal of Steel Resarch. 57:221–252.

Woghiren CO, Brennan FP., 2009. Weld toe stress concentrations in multi planar stiffened tubular KK Joints. International Journal of Fatigu. 31:164–172.

Wordsworth AC, Smedley GP., 1978. Stress concentrations at unstiffened tubular joints. Proceedings of the European Offshore Steels Research Seminar, Paper 31, Cambridge, UK.

Wordsworth AC., 1981. Stress concentration factors at K and KT tubular joint. Proceedings of the Conference on Fatigue of Offshore Structural Steels. London, UK.